Influence of Self-Gravity on the Runaway Instability of Black-Hole–Torus Systems

Pedro J. Montero,[1] José A. Font,[2] and Masaru Shibata[3]

[1]*Max-Planck-Institute für Astrophysik, Karl-Schwarzschild-Strasse 1, 81748, Garching bei München, Germany*
[2]*Departamento de Astronomía y Astrofísica, Universidad de Valencia, Dr. Moliner 50, 46100 Burjassot, Spain*
[3]*Yukawa Institute of Theoretical Physics, Kyoto University, Kyoto 606-8502, Japan*

(Received 30 October 2009; published 10 May 2010)

Results from the first fully general relativistic numerical simulations in axisymmetry of a system formed by a black hole surrounded by a self-gravitating torus in equilibrium are presented, aiming to assess the influence of the torus self-gravity on the onset of the runaway instability. We consider several models with varying torus–to–black-hole mass ratio and angular momentum distribution orbiting in equilibrium around a nonrotating black hole. The tori are perturbed to induce the mass transfer towards the black hole. Our numerical simulations show that all models exhibit a persistent phase of axisymmetric oscillations around their equilibria for several dynamical time scales without the appearance of the runaway instability, indicating that the self-gravity of the torus does not play a critical role favoring the onset of the instability, at least during the first few dynamical time scales.

DOI: 10.1103/PhysRevLett.104.191101 PACS numbers: 04.25.D−

Introduction.—Self-gravitating tori orbiting black holes (BHs) may form after the merger of a binary system formed by a BH and a neutron star (NS) or the system formed by two NS (see, e.g., [1] and references therein). In addition, they may also be the result of the gravitational collapse of the rotating core of massive stars [2,3]. State-of-the-art numerical simulations have started to provide quantitative estimates of the viability of such systems to form [1,4–11]. As such BH-torus systems are thought to be the central engine for γ-ray bursts (GRBs) [12,13], understanding its formation, dynamics, and stability properties is of high relevance.

In particular, the so-called runaway instability, first found by Abramowicz, Calvani, and Nobili [14], is an axisymmetric instability that could destroy the torus on dynamical time scales. In a marginally stable torus, the radial pressure gradient may drive the transfer of mass towards the BH through the cusplike inner edge of the torus. Because of the accretion of mass and angular momentum, both the mass of the BH and its spin increase, and the gravitational field changes, leading to two possible evolutions: (i) if the cusp moves inwards towards the BH, the mass transfer slows down and the system is stable, or (ii) if the cusp moves deeper into the torus, mass accretion will increase, and the accretion process will be runaway unstable.

The numerical study of the runaway instability has so far been investigated under different approximations (see, e.g., [15,16]). Abramowicz *et al.* [14], assuming a pseudo-Newtonian potential for the BH, constant angular momentum distribution in the torus, and an approximate treatment of the disk's self-gravity, found that the instability occurs for a wide range of initial models. More detailed studies based on stationary models, either assuming a pseudo-Newtonian potential for the BH [17] or being fully relativistic calculations [18], indicated that the self-gravity of the disk favors the instability, by arguing that, as a result of the accretion process, the cusp would move closer to the center of the torus than in non–self-gravitating disks. However, there are additional parameters which have a stabilizing effect: (i) the rotation of the BH [19], and (ii) the most important one, the radial distribution of specific angular momentum, increasing with the radial distance [20].

The first time-dependent, general relativistic hydrodynamical (GRH) axisymmetric simulations of the runaway instability were performed by Font and Daigne [15,16]. The BH evolution was assumed to follow a sequence of stationary BH spacetimes of increasing mass and angular momentum, controlled by the mass and angular momentum transferred from the torus, whose self-gravity was neglected. The first work [15], which focused on tori with constant distribution of specific angular momentum $l \equiv -u_\varphi/u_t$, with u_φ and u_t being the corresponding components of the four-velocity u_μ, showed that the system is runaway unstable on a dynamical time scale. On the other hand, the second work [16] showed that thick disks with nonconstant specific angular momentum distributions, increasing outwards with the radial distance according to a power law $l = Kr^\alpha$, are stable for very small values of the angular momentum slope α (much smaller than the Keplerian value $\alpha = 0.5$), confirming the prediction of stationary studies.

Despite the progress that has been made the existing works are still not conclusive, mainly due to the absence of important physics in the modeling. The complexity of handling the presence of a spacetime singularity in addition to the hydrodynamics and the self-gravity of the accretion torus, make full GRH simulations of such systems very challenging. The simulations presented in this Letter accomplish the goal of assembling this important

physics to provide a conclusive answer about the likelihood of the instability on the first few dynamical time scales, which cause the most concern in the context of models of short GRB. Although we do not exclude the onset of the instability on much longer time scales, it is only meaningful in connection with other relevant instabilities, specially the magnetorotational instability.

Numerical setup.—The numerical simulations have been carried out with the NADA code (see [21] for details and tests) which solves the Einstein equations (using the BSSN approach, the ''cartoon'' method, and the moving puncture approach) coupled to the GRH equations (solved with a high-resolution shock-capturing scheme based on third-order piecewise parabolic method reconstruction and the Harten-Lax-van Leer-Einfeldt approximate Riemann solver). In addition, we use a standard Γ-law equation of state (EOS), for which the pressure is expressed as a function of the rest-mass density and specific internal energy as $P = \rho\epsilon(\Gamma - 1)$, where Γ is the adiabatic exponent. For the vacuum region outside the torus we use a dynamically unimportant artificial atmosphere with rest-mass density $\rho_{\rm thr} \sim 10^{-8}\rho_{\rm max}$. The evolution equations are integrated by the method of lines, for which we use a fourth-order Runge-Kutta scheme. For the simulations reported here we use an equidistantly spaced (x, z) grid with a grid spacing $\Delta x = \Delta z = 0.05M_{\rm BH}$ and $N_x \times N_z = 600 \times 600$ points to cover a computational domain, $0 \le x \le L$ and $0 \le z \le L$, with $L = 30M_{\rm BH}$. Unless otherwise stated we use units in which $c = G = M_\odot = 1$.

Initial data.—Compact equilibrium configurations for a BH-torus system are obtained in the moving puncture framework (we refer to [22] for details). We adopt a $\Gamma = 4/3$ polytropic EOS to mimic a degenerate relativistic electron gas, and construct initial configurations using either constant or nonconstant specific angular momentum distributions, defined as $j \equiv hu_\varphi$ (h being the specific enthalpy). A list of the models along with their main features is given in Table I. We consider four different tori around a nonrotating BH (of mass $M_{\rm BH} = M_\odot$). Following [15,16,23], the EOS polytropic constant κ is chosen such that the torus-to-BH mass ratio, $M_t/M_{\rm BH}$, is 0.1, 0.5, or 1, depending on the model. We note that existing simulations of NS-NS and BH-NS mergers [1,5,7,9,24] yield $M_t \sim (0.01$–$0.2)M_\odot$. As these configurations are not overflowing the cusp, we introduce an initial perturbation to induce a small mass transfer through the inner edge of the tori (as in [23]). In our simulations we simply perturb the v^x component of the three-velocity of the torus as $v^x \approx -\eta$, which otherwise would initially be zero. For each model the numerical simulations are stopped at $t \sim 2000$, which corresponds to $\sim$10 ms (between 8 to 10 orbital periods depending on the model), since at late times the growth of the Hamiltonian constraint violation would lead to a loss of accuracy for the spacetime evolution. Nevertheless, the time scale we are considering in our simulations would allow us to identify the runaway instability, if present, as it could even take place within one orbital period for the more massive models M2 and M4 (see [15,16]).

TABLE I. Main properties of the equilibrium models studied in units of $c = G = M_\odot = 1$ (unless shown otherwise). From left to right the columns show: the type of specific angular momentum distribution, the torus-to-BH mass ratio, the position of the maximum density point $r_{\rm max}$, the position of the inner and outer radii of the torus $r_{\rm in}$ and $r_{\rm out}$, the maximum rest-mass density, and the orbital period at the center of the torus $t_{\rm orb}$.

Model	j law	$M_t/M_{\rm BH}$	$r_{\rm max}$	$r_{\rm in}$	$r_{\rm out}$	$\rho_{\rm max}$ (g/cm^3)	$t_{\rm orb}$
$M1$	const	0.1	7.17	4.92	10.17	3.189×10^{14}	147.81
$M2$	const	1.0	8.87	4.02	19.97	2.202×10^{14}	199.54
$M3$	nonconst	0.1	10.47	4.92	19.97	3.902×10^{13}	245.37
$M4$	nonconst	0.5	10.02	4.07	19.97	1.538×10^{14}	229.91

Results.—The left panel in Fig. 1 displays the time evolution of the total rest mass and central rest-mass density, each of them normalized to its initial value, for the evolution of models $M1$ (solid and dashed lines) and $M2$ (dotted line). $M1$ is a model with j constant and with an initial rest mass of $M_t = 0.1M_{\rm BH}$, thus representing a model with torus-to-BH mass ratio in agreement with results obtained by simulations of NS-NS or BH-NS mergers [1,5,7,9,24]. For this initial model, we have considered two different initial perturbations, $\eta = 0.01$ (solid line) and $\eta = 0.025$ (dashed line), to evaluate its influence on the overall dynamics. As expected, the initial perturbation triggers a phase of axisymmetric oscillations of the torus around its equilibrium which are present throughout the simulation. Such oscillations induce a small outflow of matter through the cusp towards the BH. This, however, does not reduce significantly the total rest mass of the torus, plotted in the upper panel. At the end of the simulation ($t \sim 10t_{\rm orb}$) the rest mass of the torus $M1$ is conserved up to about 1%. Therefore, the BH mass and spin do not increase with time significantly, and the torus shows no sign of the runaway instability. Further information about the process of accretion is obtained from the right panel in Fig. 1, which shows the time evolution of the mass accretion rate. We notice that the mass accretion rate for model $M1$ is larger the larger the initial perturbation is. For $\eta = 0.025$, there is an initial stage of very small mass transfer through the inner edge of the torus which lasts for about half an orbit ($t \sim 80$). This is followed by a stage in which the oscillatory behavior of the rest-mass accretion rate, signature of the induced oscillations, is obvious throughout the numerical evolution. Interestingly, during the oscillation phase, the mass flux does not increase in amplitude with time, as one would expect prior to the onset of the runaway instability (see [15,16]). Instead, it reaches a maximum of about $\dot{M} \sim 0.1M_\odot/$s after the second orbital period. Later it decreases and exhibits a series of oscillations around a lower value, never showing any signature of exponential growth. The mass accretion rates of the perturbed tori are in good agreement with the maximum expected accretion rates for hyperaccreting disks associ-

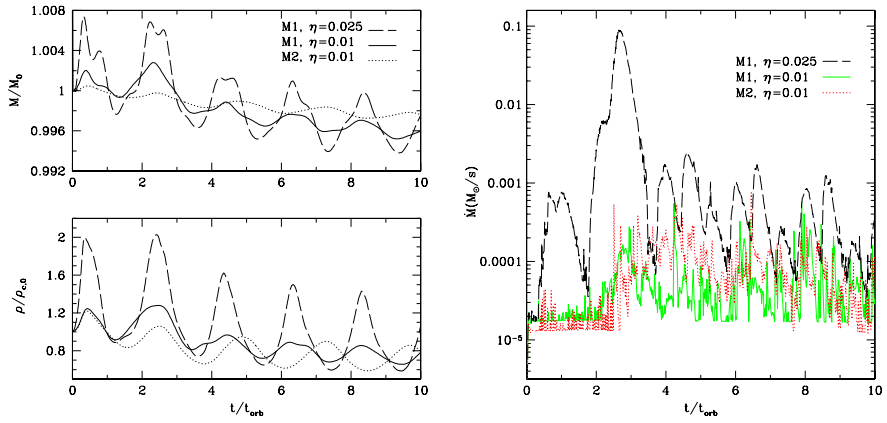

FIG. 1 (color online). Left panel: Time evolution of the total rest-mass (top) and central rest-mass density, each of them normalized to its initial value, for the evolution of models *M1* and *M2*. Right panel: Mass accretion rate evolution for models *M1* and *M2*.

ated with the central engine of γ-ray bursts, which could be as high as $\dot{M} \sim (0.01\text{–}1)M_\odot/\mathrm{s}$, depending on the formation mechanism [25]. In the case of a disk formed by the merger of a NS with another compact object (either a NS or a BH), most of the material in the accretion disk would be accreted on a time scale comparable to the viscous time scale $t_{\mathrm{visc}} \sim 0.1$ s. In the collapsar scenario, such high accretion rates could be sustained for $\sim$10 s as the disk is fed by the infalling stellar material.

We consider next a significantly more massive torus, model *M2*, while keeping the same rotation law. The total rest mass of this torus is $M_t = 1.0M_{\mathrm{BH}}$. We use a small initial perturbation, $\eta = 0.01$, because due to the larger coordinate dimension of the torus, a larger perturbation would cause its outer parts to move outside the computational domain. Despite being more massive the overall dynamics of *M2* is very similar to the one discussed above for the less massive torus, *M1*. As expected, the time evolution of the central rest-mass density, displayed in the left panel of Fig. 1 with a dotted line, shows a series of axisymmetric oscillations during the entire length of the simulation. As we have observed for the low mass torus, the amplitude in the evolution of the mass flux does not increase with time and does not lead to the onset of the instability.

We note that these results do not actually contradict results obtained for non-self-gravitating tori with constant distribution of angular momentum [15]. Notice that despite the difference in the definition of the specific angular momentum, the j-constant condition in our models leads to constant l up to a difference of the order of 10^{-5}. In addition, models of [15] and the ones considered here satisfy the condition $j_{\mathrm{torus}} > j_{\mathrm{ISCO}}$ throughout the evolution, where ISCO stands for innermost stable circular orbit. However, those previous studies considered initial models which were overflowing the cusp in order to induce a large stationary accretion rate, which varied between $\dot{M} \sim (0.1\text{–}34.0)M_\odot/\mathrm{s}$. Unstable runaway behavior in the case of mass accretion rates of $\dot{M} \sim 0.1M_\odot/\mathrm{s}$ were found on a time scale of 100 t_{orb}, and only on a dynamical time scale for the largest values of the mass flux. Similar results were found by [23] introducing an initial perturbation on the equilibrium tori. Since in our case $\dot{M} \sim (10^{-3}\text{–}10^{-4})M_\odot/\mathrm{s}$ throughout the simulations, the exponential growth of the mass accretion would not manifest itself even on such time scales. This is in agreement with the recent work of [1] where a systematic study of the BH-torus systems produced by the merger of unequal-mass NS binaries was presented, concluding that self-gravitating tori with mass accretion rates as high as $\dot{M} \sim 2.0M_\odot/\mathrm{s}$ were stable on the dynamical time scales investigated.

Motivated by the influence of different rotation laws on the onset of the instability [15] we have also carried out numerical evolutions of two j-non-constant models, *M3* and *M4*, with two different torus-to-BH mass ratios, 0.1 and 0.5, respectively. Despite the difference in the rotation law with respect to models *M1* and *M2*, the dynamics is very similar, as inferred from the evolution of the mass accretion rate displayed in Fig. 2. No exponential growth of the mass flux is found and, therefore, no runaway instability is present.

Studies [17,18] mainly based on stationary models, either assuming a pseudo-Newtonian potential for the BH and a Newtonian potential for the self-gravity of the torus, or being fully relativistic calculations indicated that the self-gravity of the disk favors the instability. The simulations presented here overcome the limitations of preceding works. Our results indicate that in the general case in which mass accretion rates are consistent with those expected for hyperaccreting disks, and in which the angular momentum distribution increases with the radial distance, the effect of self-gravity is not sufficient to lead to unstable accretion.

Despite the simplifying assumptions of our models (magnetic fields or detailed microphysics are not considered), our results are consistent with the expected dynamics and mass accretion rates for hyperaccreting disks and do not challenge the time scale required for producing a GRB. Moreover, although magnetic fields have not been considered in our simulations, it is likely that these do not play a critical role in the context of the runaway instability.

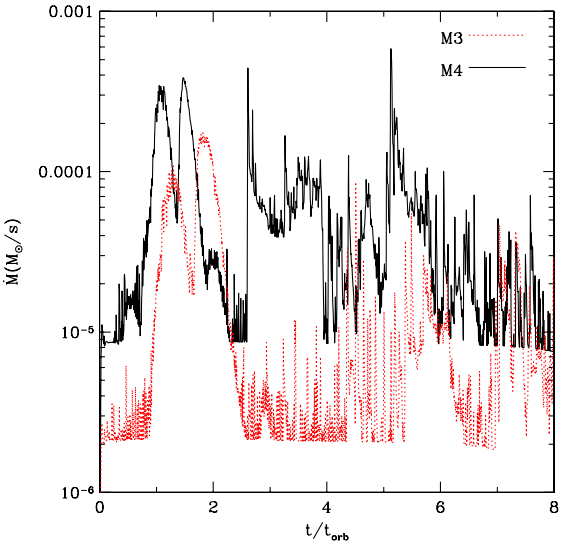

FIG. 2 (color online). Mass accretion rate for models *M3* and *M4*.

Despite the fact that numerical simulations of magnetized NS mergers are still scarce and the results are inconclusive, simulations by [26] indicate that the effect of the magnetic fields during the merger and the initial phase of the BH-torus lifetime is not dramatic (as reflected by the similarities between the gravitational waves in the magnetized and unmagnetized cases), rather these are expected to become more important during the secular evolution of the accretion torus.

Conclusions.—We have presented results from the first fully general relativistic numerical simulations in axisymmetry of a system formed by a BH surrounded by a marginally stable self-gravitating torus aiming to assess the influence of the torus self-gravity on the onset of the runaway instability. Several models with different torus-to-BH mass ratio and angular momentum distributions have been considered. The tori have been perturbed to induce mass transfer towards the BH. Our numerical simulations show that all models exhibit a persistent phase of axisymmetric oscillations around their equilibria for several dynamical time scales without the appearance of the runaway instability. Thus, the self-gravity of the torus does not play a critical role favoring the onset of the instability. Clearly, to investigate additional $m = 1$ nonaxisymmetric features that may play a role on the dynamics of the system 3D simulations are required. Nevertheless, the robustness of our results in axisymmetry on the influence of self-gravity on the runaway instability are confirmed by simulations we have also performed with the independent 2D code of [27]. These simulations and the investigation of nonaxisymmetric instabilities of self-gravitating tori around BHs will be presented elsewhere.

We thank Frederic Daigne, Ewald Müller, and Yudai Suwa for useful comments. This work was supported by the Collaborative Research Center on Gravitational Wave Astronomy of the Deutsche Forschungsgesellschaft (DFG SFB/Transregio 7), the Spanish Ministerio de Educación y Ciencia (AYA 2007-67626-C03-01) and by a Grant-in-Aid for Scientific Research (21340051) and by a Grant-in-Aid for Scientific Research on Innovative Area (20105004) of the Japanese Monbukagakusho.

[1] L. Rezzolla, L. Baiotti, B. Giacomazzo, D. Link, and J. A. Font, arXiv:1001.3074.
[2] S. E. Woosley, Astrophys. J. **405**, 273 (1993).
[3] B. Paczynski, Astrophys. J. Lett. **494**, L45 (1998).
[4] M. Shibata, K. Taniguchi, and K. Uryu, Phys. Rev. D **71**, 084021 (2005).
[5] M. Shibata and K. Taniguchi, Phys. Rev. D **73**, 064027 (2006).
[6] M. Shibata and K. Uryu, Phys. Rev. D **74**, 121503(R) (2006).
[7] M. Shibata, M. D. Duez, Y. T. Liu, S. L. Shapiro, and B. C. Stephens, Phys. Rev. Lett. **96**, 031102 (2006).
[8] M. Shibata and K. Uryu, Classical Quantum Gravity **24**, S125 (2007).
[9] L. Baiotti, B. Giacomazzo, and L. Rezzolla, Phys. Rev. D **78**, 084033 (2008).
[10] M. Duez, F. Foucart, L. E. Kidder, C. D. Ott, and S. A. Teukolsky, arXiv:0912.3528.
[11] Z. B. Etienne, Y. T. Liu, S. L. Shapiro, and T. W. Baumgarte, Phys. Rev. D **79**, 044024 (2009).
[12] T. Piran, Phys. Rep. **314**, 575 (1999).
[13] P. Meszaros, Rep. Prog. Phys. **69**, 2259 (2006).
[14] M. A. Abramowicz, M. Calvani, and L. Nobili, Nature (London) **302**, 597 (1983).
[15] J. A. Font and F. Daigne, Mon. Not. R. Astron. Soc. **334**, 383 (2002).
[16] F. Daigne and J. A. Font, Mon. Not. R. Astron. Soc. **349**, 841 (2004).
[17] R. Khanna and S. K. Chakrabarti, Mon. Not. R. Astron. Soc. **259**, 1 (1992); N. Masuda, S. Nishida, and Y. Eriguchi, Mon. Not. R. Astron. Soc. **297**, 1139 (1998).
[18] S. Nishida, A. Lanza, Y. Eriguchi, and M. A. Abramowicz, Mon. Not. R. Astron. Soc. **278**, L41 (1996).
[19] D. B. Wilson, Nature (London) **312**, 620 (1984).
[20] F. Daigne and R. Mochkovitch, Mon. Not. R. Astron. Soc. **285**, L15 (1997); M. A. Abramowicz, V. Karas, and A. Lanza, Astron. Astrophys. **331**, 1143 (1998).
[21] P. J. Montero, J. A. Font, and M. Shibata, Phys. Rev. D **78**, 064037 (2008).
[22] M. Shibata, Phys. Rev. D **76**, 064035 (2007).
[23] O. Zanotti, L. Rezzolla, and J. A. Font, Mon. Not. R. Astron. Soc. **341**, 832 (2003).
[24] M. Shibata, K. Kyutoku, T. Yamamoto, and K. Taniguchi, Phys. Rev. D **79**, 044030 (2009).
[25] W. Chen and A. M. Beloborodov, Astrophys. J. **657**, 383 (2007).
[26] Y. T. Liu, S. L. Shapiro, Z. B. Etienne, and K. Taniguchi, Phys. Rev. D **78**, 024012 (2008).
[27] M. Shibata, Phys. Rev. D **67**, 024033 (2003).